FWM Wavelength Conversion Analysis in a 3-Integrated Portion SOA and DFB Laser using Coupled Wave Approach and FD-BPM Method

M. K. Moazzam, A. Salmanpour, M. Nirouei

Abstract—In this paper we have numerically analyzed terahertz-range wavelength conversion using nondegenerate four wave mixing (NDFWM) in a SOA integrated DFB laser (experiments reported both in MIT electronics and Fujitsu research laboratories). For analyzing semiconductor optical amplifier (SOA), we use finite-difference beam propagation method (FDBPM) based on modified nonlinear Schrödinger equation and for distributed feedback (DFB) laser we use coupled wave approach. We investigated wavelength conversion up to 4THz probe-pump detuning with conversion efficiency -5dB in 1THz probe-pump detuning for a SOA integrated quantum-well λ/4-shifted DFB laser. We have successfully estimated for the first time FWM conversion efficiency in the tested device. This result compared with experiment measurements demonstrates suitable compatibility.

Keywords—distributed feedback laser, nondegenerate four wave mixing, semiconductor optical amplifier, wavelength conversion

I. INTRODUCTION

IN recent years, WDM optical communication systems has assigned themselves a broad width of optical networks; which the most important element has been used in them is the wavelength converter [1]-[4]. Besides, with increasing data communication rate in optical fiber, the demand to extra high velocity devices, which are the same full optical devices, is an unavoidable demand. In order to design such full optical wavelength converters, much efforts has been done, which one of the best made compositions is the SOA integrated DFB laser [1]. This device with excellent features, like format- free and broad band wavelength conversion, polarization independence operation using the dual-pump technique and more important than all, extra excellent conversion efficiency, is from devices that has attracted many attentions [1] and [5]. In this paper, we investigate nondegenerate four wave mixing (NFWM) and the conversion efficiency due to it for wavelength conversion in a SOA (semiconductor optical amplifier) integrated DFB (distributed feedback) laser. As
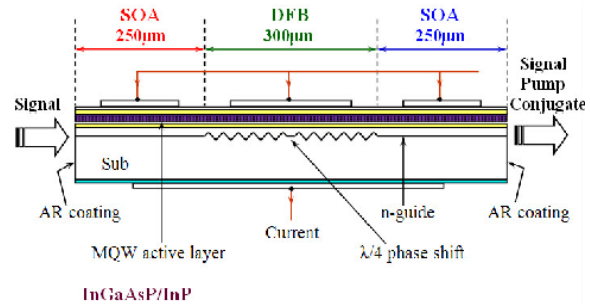
M. K. Moazzam is with Guilan University, Rasht, Iran (phone: +98-131-6690577; fax: +98-131-6690577; e-mail: mkmoazzam@yahoo.com).

A. Salmanpour was with Electrical Engineering Department of AZAD University-Lahijan Branch. He is now with Guilan Power Distribution Company, Rasht, Iran (phone: +98-131-6665001; fax: +98-131-6664499; e-mail: ar.salmanpour@yahoo.com).

M. Nirouei is with Electrical Engineering Department of AZAD University-Lahijan Branch, Iran (phone: +98-131-7730352; fax: +98-131-7720327; e-mail: mahyar.n@gmail.com).

Fig. 1 The λ/4-phase-shift DFB laser with SOA integration

shown in Fig. 1 [7], our integrated device [1] has been composed of three portions. Input-side SOA (left-side SOA) part, which in order to increase device linear gain has been added to device; and, the output-side SOA portion which has a fundamental role in wavelength conversion has been assigned to this wavelength converter to increase conversion efficiency more and more. In order to analyze these two portions and to investigate the amount of the effect of these on the integrated device conversion efficiency, we use finite-difference beam propagation method (FD-BPM) [6]. The central part of the integrated device is a quarter-wave-shifted distributed feedback (QWS-DFB) laser, which using NDFWM, terahertz wavelength conversion can be resulted in this device. We use coupled wave approach to investigate the amount of the efficiency result of this portion in integrated device wavelength conversion [7] and [8]. Using two above models together, we can simulate a tested integrated device successfully.

II. ANALYTICAL MODELING

A. Analytical Model for SOA Portion

The model main equation that is derived from wave equation is the modified nonlinear Schrödinger equation which for a single optical pulse with considering of slowly varying envelope approximation access is as follows [5] and [9]:

$$[\frac{\partial}{\partial z} - \frac{i}{2}\beta_2 \frac{\partial^2}{\partial \tau^2} + \frac{\gamma}{2} + (\frac{\gamma_{2p}}{2} + ib_2)|V(\tau,z)|^2]V(\tau,z)$$

$$= \{\frac{1}{2}g_N(\tau)[\frac{1}{f(\tau)} + i\alpha_N] + \frac{1}{2}\Delta g_T(\tau)(1 + i\alpha_T) \quad (1)$$

$$-i\frac{1}{2}\frac{\partial g(\tau,\omega)}{\partial \omega}\Big|_{\omega_0}\frac{\partial}{\partial \tau} - \frac{1}{4}\frac{\partial^2 g(\tau,\omega)}{\partial \omega^2}\Big|_{\omega_0}\frac{\partial^2}{\partial \tau^2}\}V(\tau,z).$$

Where $V(\tau, z)$ is the time domain complex envelope function of an optical pulse in local time frame $\tau (= t - z / v_g)$; which v_g is group propagation velocity in center frequency of optical Pulse. Besides, $|V(\tau, z)|^2$ is the representative of optical pulse Power. In left side of this equation, β_2 is group velocity dispersion (GVD), γ is the linear loss, γ_{2p} is the two-photon absorption coefficient, $b_2 (= \omega_0 n_2 / cA)$ is the instantaneous self-phase modulation term, $\omega_0 (= 2\pi f_0)$ is the center angular frequency of the pulse, n_2 is the instantaneous nonlinear refractive index, c is the velocity of light in vacuum, and $A (= wd / \Gamma)$ is effective area which, w and d are its width and thickness of the active area, respectively, and Γ is the confinement factor.

The first part of right hand side of (1) represents dynamic gain due to carrier density variations N; where $g_N(\tau)$ and α_N are the saturated gain and the line width enhancement factor due to carrier depletion, respectively, $f(\tau)$ is spectral hole-burning function (SHB). Also, In the second part of the right side of (1), which represents gain dynamics due to variations of carrier temperature, $\Delta g_T(\tau)$ is gain changes due to the carrier heating and two-photon absorption and α_T is the line width enhancement factor due to the carrier heating. And finally, the last two part of MNSE, are gain and phase dynamic dispersion model, respectively, which full model is as developed in [9].

For simulation of above model, we use FD-BPM technique. With this approach, the tridiagonal simultaneous linear equations system is resulted, which with solving them in each propagation position z, we can find the complex envelope function of optical pulse in the next position $V(z + \Delta z)$, which Δz is propagation step. We have used the following equation for describing the three input pulses, which are simultaneously injected into the SOA:

$$V(\tau) = V_p(\tau) + V_q(\tau) \exp(-i\Delta\omega\tau) + V_{cc}(\tau) \exp(i\Delta\omega\tau) \quad (2)$$

Where $V_p(\tau)$, $V_q(\tau)$ and $V_{cc}(\tau)$ are the complex envelope functions of the input pump, probe and conjugate pulses, and $\Delta\omega$ is a detuning angular frequency:

$$\Delta\omega = 2\pi\Delta f = 2\pi(f_p - f_q) = 2\pi(f_{cc} - f_p) \quad (3)$$

In order to investigate FWM efficiency in left-side SOA, we solve (1) using combined envelope function (2) by iterative approximation technique [6].

B. Theoretical Model for DFB Laser Portion

The model which we utilize for DFB portion is coupled wave model [7] and [8]. The intra-cavity TE-polarized and normalized electrical field in a QWS-DFB laser can be written

as follows:

$$E(z,t) = \exp(-i\omega_j t) \sum_{j=0,1,2} [R_j(z)\exp(ik_B z) + S_j(z)\exp(-ik_B z)] + cc. \quad (4)$$

where R_j and S_j are the complex slowly varying envelope functions of the forward and backward fields, respectively; j=0,1 and 2 are representatives of produced inner pump wave in laser, probe wave and produced conjugate wave due to FWM phenomena, respectively. $k_B (= \pi / \Lambda)$ is the Bragg wave number, and Λ is the first-order index grating period. With substituting (4) in the wave equation, bellow coupled wave equations for a DFB laser cavity are obtained [7]:

$$\frac{dR_j}{dz} = [\frac{i\omega_j^2 \Gamma \chi_j^L}{2k_B c^2} + \frac{i(k_j^2 - k_B^2)}{2k_B}]R_j + (\frac{i\kappa k_j}{k_B})S_j$$
$$+ \frac{i\omega_j^2 \Gamma \chi_j^{FWM}}{2k_B c^2 E_0^2}[R_0^2 R_{3-j}^* + 2R_0 S_0 S_{3-j}^*]$$
$$-\frac{dS_j}{dz} = [\frac{i\omega_j^2 \Gamma \chi_j^L}{2k_B c^2} + \frac{i(k_j^2 - k_B^2)}{2k_B}]S_j + (\frac{i\kappa k_j}{k_B})R_j \quad (5)$$
$$+ \frac{i\omega_j^2 \Gamma \chi_j^{FWM}}{2k_B c^2 E_0^2}[S_0^2 S_{3-j}^* + 2R_0 S_0 R_{3-j}^*]$$

Where, the boundary conditions at the end facets of DFB are:

$$R_1(z=0) = A_{inj}, \quad R_2(z=0) = 0, \quad S_{1,2}(z=0) = 0 \quad (6)$$

In above equations, where ω_j is the angular frequency of the jth wave, Γ is the confinement factor, κ is the DFB coupling coefficient, $k_j (= \bar{n}_j \omega_j / c)$ is the wave number of the jth wave and $\bar{n}_j$ is the effective mode index.

After solving (5) numerically, the transmission and reflection gains of probe and conjugate waves are calculated by bellow relations:

$$Tra_{1,2} = |R_{1,2}(L)|^2 / |A_{inj}|^2 \quad (7)$$

$$Ref_{1,2} = |S_{1,2}(0)|^2 / |A_{inj}|^2 \quad (8)$$

In this paper, we use listed values of parameters in table I to simulate different portions of considered integrated device [7], [8], and [12].

III. RESULT AND DISCUSSION

A. Left Side SOA Portion (input-side SOA)

Our considered device is a device that pump pulse is produced in its central DFB portion in an inner manner; so, input side SOA portion will be injected with only one input single probe pulse. The shape of input pulse of our model is

$sech^2$ and has limited Fourier transformation. In order to coincide the results obtained from simulation and empirical results, the duration of input pulse has been considered 40 ps [6]. For such duration of pulse, sampling time should be 62.5 fs and sampling frequency should be 3.90625 GHz. The power of probe pulse has been considered -22 dBm; with respect to duration of pulse, its energy will be 0.25 fJ. With this input energy, the efficiency obtained from left side SOA portion is 3.42 dB, which has been earned without device gain saturation.

B. Central DFB Laser Portion

The descried model for DFB laser portion is established based on solving (5) under boundary conditions (6). To solve such two-point boundary values problem, the best possible choice is to use iterative Shooting algorithm [8]. In Fig. 2 and 3, the obtained conversion efficiency from the model for an isolated DFB laser device in positive and negative terahertz-range detuning (upward and downward frequency conversion) has been shown, respectively. These calculations has been done for a device with small coupling coefficient $\kappa L = 0.9$ and for some different output pump power levels, P_{outDFB}.

C. Right-Side SOA Portion (Output-side SOA)

This portion is the most important of the integrated structure; because this part functions both as an optical amplifier and also as an optical conjugator. Output powers pump-probe and the FWM signal which go out of DFB laser portion, should be injected to this portion. The duration of each three input pulse to this section is considered 40 ps, like left-side SOA. The energy of each of these pulses is specified by related output power of DFB portion. Input pump pulse energy is considered fixed and equals to 0.56 pJ. At first, we compare the obtained results from the model with experimental data. To do so, the conversion efficiency obtained from simulation for a full device, versus positive and negative detuning, has been shown with open circles in fig. 4 and 5, respectively. These results, for a device with $\kappa L = 1.8$ and also for some different normalized pump power level (P_{out} / P_s) for DFB portion have been calculated. As observed, with listed parameters in table I ([2]-[7], [11], and [12]) and in DFB output pump power $P_{outDFB} = 1.4 P_s$, we can reach the best fitting between simulation and experimental results [1]. It is important to note that this output pump power level for DFB portion, after being amplified in output SOA portion, will be equaled to 14.7 dBm in full integrated device output. In Fig. 6, the conversion efficiency of a full integrated structure with previous mentioned characteristics (and output pump level $P_{out} = 1.4 P_s$ for DFB portion), and also for comparison that of an integrated device without output SOA has been shown. As shown in this figure output SOA portion improves the conversion efficiency 10-15 dB. On the other hand, also in Fig. 6 and for comparison, the conversion efficiency of an integrated device without input SOA portion

TABLE I
LIST OF THE PARAMETERS USED IN SIMULATION

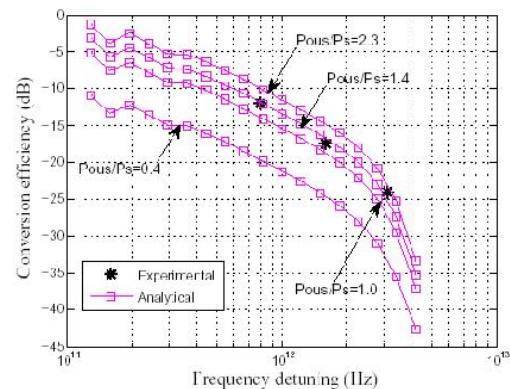| Symbols	Values	Units
L_{SOA}	250	μm
L_{DFB}	300	μm
A	0.21	μm^2
f_0	193	THz
β_2	0.07	$ps^2 cm^{-1}$
α_N	3.4	
α_T	2.1	
γ	10.5	cm^{-1}
n_2	−0.5	$cm^2 TW^{-1}$
γ_{2p}	25	$cm^{-1} GW^{-1}$

Fig. 2 Analytical and experimental FWM conversion efficiency of an isolated DFB laser versus positive terahertz-range detuning (upward frequency conversion). The rectangles are Analytical results and the stars are experimental data [1] and [9].
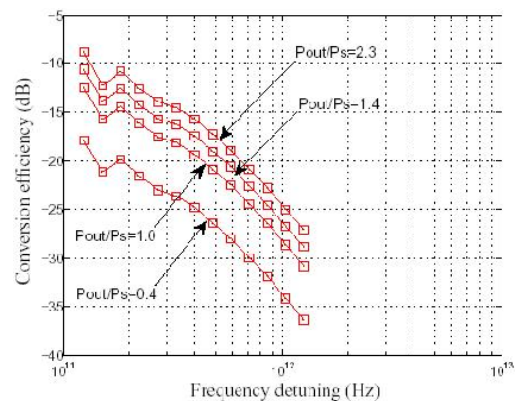

Fig. 3 Analytical FWM conversion efficiency of an isolated DFB laser versus negative terahertz-range detuning (downward frequency conversion)

in the same detuning band has been figured with open circles. As we expect, the conversion efficiency of the full device is more and this difference is 3.4 dB. By comparing diagrams of Fig. 6, it is obvious that the output SOA portion has a more important role rather than input SOA portion in improving of device conversion efficiency; so that for a device with mentioned features, output-side SOA increases the conversion

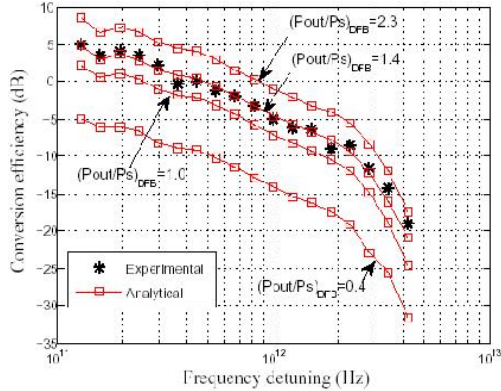efficiency of the integrated device 6.3 time as much as input-side SOA.

Fig. 4 Analytical and experimental FWM conversion efficiency of a SOA integrated DFB laser (full device) versus positive detuning (upward frequency conversion). The rectangles are Analytical results and the stars are experimental data
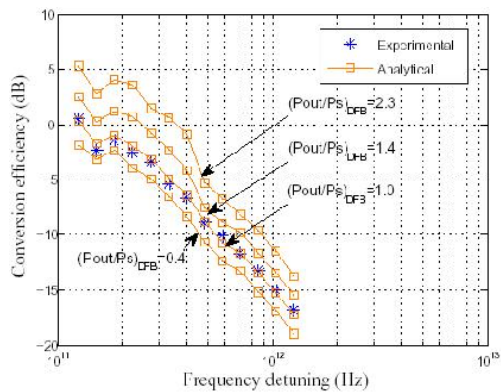

Fig. 5 Analytical and experimental FWM conversion efficiency of a SOA integrated DFB laser (full device) versus negative detuning (downward frequency conversion). The rectangles are Analytical results and the stars are experimental data

IV. CONCLUSION

In this paper, we represented a numerical analysis of nondegenerated four wave mixing (NFWM) in terahertz-range for a device of SOA integrated QWS-DFB laser. In order to Investigate wavelength conversion, in λ/4 central shifted DFB laser portion; we used coupled wave approach. We used finite difference beam propagation method to analyze the behavior of two sections of the SOA which has been added to the central part to increase device conversion efficiency. From the high assimilation of numerical results, due to simulation, and the empirical data, this paper quantitatively shows that our composed model is very useful and robust to analyze FWM features in a SOA device integrated with a QWSDFB laser. Moreover, the device treatment in wavelength conversion without presence of any input or output sections was analyzed. We observed that the conversion efficiency of the integrated device depended on SOA output section increasingly. We hope that our results can improve designing and performance of high
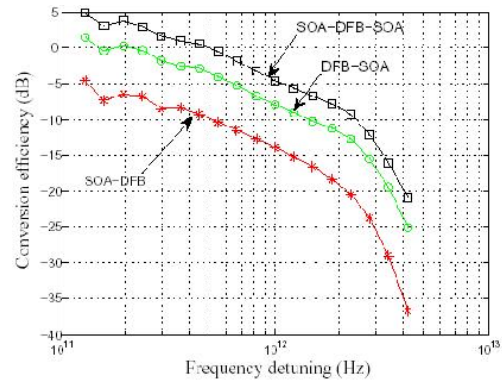

Fig. 6 FWM conversion efficiency versus positive detuning (upward frequency conversion). The rectangles are conversion efficiency for a full device. The circles are conversion efficiency for an integrated device without input SOA portion. The stars are conversion efficiency for an integrated device without output SOA portion

efficiency wavelength converters, wavelength division multiplexers, and especially current WDM systems, which function in optical networks using integrated SOA-DFB wavelength converters.

REFERENCES

[1] T. Simoyama, H. Kuwatsuka, M. Matsuda, Y. Kotaki, and H. Ishikawa,"High-efficiency wavelength conversion using FWM in an SOA integrated DFB laser," IEEE Photon. Technol. Lett., vol. 12, pp. 31-33, 2000.
[2] P. M. Gong, J. T. Hsieh, S. L. Lee, and J. Wu, "Theoretical Analysis of Wavelength Conversion Based on Four-Wave Mixing in Light-Holding SOAs," IEEE J. Quantum Electron., vol. 40, pp. 31-40, Jan. 2004.
[3] C. Politi, D Klonidis, and M. J. OMahony, "Dynamic Behavior of Wavelength Converters Based on FWM in SOAs," IEEE J. Quantum Electron., vol. 42, pp. 108-125, Feb. 2006.
[4] J. T. Hsieh, P. M. Gong, S. L. Lee, and J. Wu, "Improved Dynamic Characteristics on Four-Wave Mixing Wavelength Conversion in Light-Holding SOAs," IEEE J. Select. Topics Quantum Electron., vol. 10, pp.1187-1196, Sep. 2004.
[5] T. Akiyama, H. Kuwatsuka, T. Simoyama, M. Sugawara and H. Ishikawa, "Design optimisation of SOA-integrated DFB laser wavelength converter," Electron. Lett., vol. 38, pp. 239-241, Feb. 2002.[6] N. Kumar Das, Y. Yamayoshi, and H. Kawaguchi, "Analysis of basic four-wave mixing characteristics in a semiconductor optical amplifier by the finite-difference beam propagation method," IEEE J. Quantum Electron.,vol. 36, pp. 1184-1192, 2000.
[6] Kaatuzian H. and Mostafa Keshavarz Moazzam "All Optical Wavelength Conversion Analytical Investigation in a FWM based SOA Integrated DFB Laser Wavelength Converter," SPIE. Optical Engineering., vol. 47(1), pp. 14202, 2008.
[7] J.W. D. Chi, K. Alan Shore, and J. Le Bihan, "Highly nondegenerate four-wave mixing in uniform and /4-shifted DFB lasers," IEEE J. Quantum Electron., vol. 33, pp. 2011-2020, 1997.
[8] T. Simoyama, H. Kuwatsuka, and H. Ishikawa, "Cavity length dependence of wavelength conversion efficiency of four-wave mixing in /4-shifted DFB laser," FUJITSU Scientific Tech. J., vol. 34, pp. 235-344, 1998.
[9] Bingbing. Wu, Songnian. Fu , and Jian. Wu "40 Gb/s Multifunction Optical Format Conversion Module With Wavelength Multicast Capability Using Nondegenerate Four-Wave Mixing in a Semiconductor Optical Amplifier," Journal of Light wave Technology, vol.27, pp.4446, 2009.
[10] J. Leuthold, M. Mayer, J. Eckner, G. Guekos, H. Melchior, and Ch. Zellweger, " Material gain of bulk 1.55 μm InGaAsP/InP semiconductor optical amplifiers approximated by a polynomial model," J. Appl. Phys., vol. 87, pp. 618-620, 2000.

[11] A. Mecozzi, S. Scotti, A. DOttavi, E. Iannone, and P. Spano, " Four wave mixing in traveling-wave semiconductor amplifiers," IEEE J. Quantum Electron., vol. 31, pp. 689699, Apr. 1995.